음향방출법(AE)에 의한 기계요소재의 마찰용접 품질 실시간 평가

오세규 회원(부산수산대학교 공대 기계공학과, 교수, 공학박사)

REAL-TIME QUALITY EVALUATION OF FRICTION WELDING OF MACHINE COMPONENTS BY ACOUSTIC EMISSION

BY SAE-KYOO OH*

-Development of Real-Time Quality Evaluation of Friction Welding by Acousitc Emission : Report 1

ABSTRACT

According as the friction welding has been increasingly applied in manufacturing various machine components because of its significant economic and technical advantages, one of the important concerns is the reliable quality monitoring method for a good weld quality with both joint strength and toughness in the process of its production. However no reliable nondestructive test method is available at present to determine the weld quality particularly in process of production.

So this paper presents an experimental examination and quantitative analysis for the real-time evaluation of friction weld quality by acoustic emission, as a new approach which attempts finally to develop an on-line quality monitoring system design for friction welds using AE techniques.

As one of the important results, it was confirmed, through this study, that AE techniques can be reliably applied to evaluating the friction weld quality with 100% joint strength, as the cumulative AE counts occurring during welding period were quantitatively correlated with reliability at 95% confidence level to the joint strength of welds.

Key Words : Quality evaluation, Friction welding, Acoustic emission, Welding condition, weld strength, cumulative total AE counts, Joint efficiency.

1. INTRODUCTION

In applying friction welding process, one of the important concerns is the reliable quality monitoring method for a good weld strength in process of production. However, no reliable nondestructive test method is available at present to monitor the weld strength quantitatively in process[1,2] except the author, et al.'s reports[3,4,5], even though studies on ultrasonic detection of weld strength were reported[6,7] but no quantitative relationship was drawn because of considerable scattering of the data.

In this continued study since the former reports[3,4,5], the relationship between the weld strength and the measurable acoustic emission total counts was analyzed quantitatively. This was possible through relating the direct measurement and analysis of AE counts to the strength (tensile strength) of friction welds of medium carbon low alloy steel bars to sulfurized free machining steel bars and stainless steel tubes to low carbon steel tubes.

2. SPECIMENS AND PROCEDURES

The dimensions of welding workpieces and tension test specimens are the same as those in Fig. 1. And the chemical compositions and tensile strength of base metals are listed in Table 1. The friction welding conditions (inertia type) used in this study are revealed in Table 2 including the diameters of workpieces.

Table 1 Chemical compositions and tensile strength of base metals.

MATERIALS (AISI)	CHEMICAL COMPOSITION (wt %)									T.S*
	C	Mn	P	S	Pb	Cr	Mo	Ni	Si	σ_T
4140	0.38	0.75	0.04	-	-	0.80	0.15	-	0.20	113.4
1117	0.17	1.00	0.04	0.08	-	-	-	-	-	72.1
12L14	0.15	0.85	0.04	0.26	0.15	-	-	-	-	66.9
1020	0.20	0.45	0.04	0.05	-	-	-	-	-	62.2
304S.S.	0.08	2.00	0.04	0.03	-	18.0	-	8.00	0.75	75.5

* Unit: kgf/mm^2, each specimen with 0.635 mm R notch.

*Professor, Dept. of Mech. Engrg., College of Engrg., Nat'l Fi. Univ. of Pusan

Table 2 Welding conditions.

MATERIALS COMBINATION (AISI)	DIAMETER D, mm	MOMENT OF INERTIA I, kgfm²	INITIAL ROTATING SPEED V, rpm	AXIAL PRESSURE p, kgf/mm²	INITIAL ENERGY E, kgfm
Bar-to-bar 4140-1117	9.525	0.118	1136	12.7	85
		0.236	937—3450		116—1572
		0.472	883—2592		206—1747
Bar-to-bar 4a ~-12L14	9.525	0.236	1132—2822	12.7	169—1052
Tube-to-tube 1020-304 SS	OD 25.40 ID 19.05	0.472	796—2984	8.2	167—2351

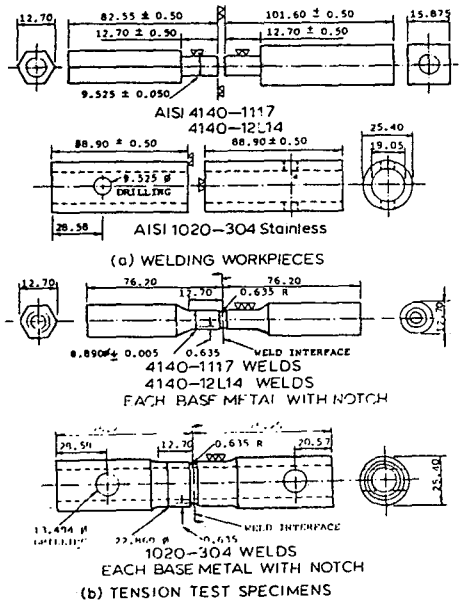

Fig.1 Welding workpieces and tension test specimens.

The AE transducer location diagram and the block diagram of electronic components for the AE monitoring equipment including the welding parameter-history measuring apparatus are given in Fig. 2-(a) and (b)[3], respectively. A 22.225 mmϕ acoustic emission piezoelectric transducer (sensitivity-65 db) was tightly mounted with tape on the jaw, using high vacuum grease on the contacting surface. At such a location as shown in Fig. 2-(a), there was no thermal effect from the interface. The AE equipment was a standard commercial unit (Dunegan/ Endevco Model 3000). As shown in Fig.2-(b), the band pass filter was set to 100 through 300kHz to remove the background noise, and AE signals were further amplified 35 db with a variable broadband amplifier (0-60db) after the preamplifier of 40 db[3]. Thereby, the total system gain setting was 75 db in this study, that is, counting each pulse that exceeded-75 dbv. About eighty workpieces for each metal pair (AISI 4140-1117, 4140-12L14, 1020-304) for welding and measuring AE counts were prepared.

Fig. 3[3] shows the typical history of welding parameters and AE measurements in inertia friction welding. The total cumulative AE counts (N, counts) at Zone A of the welding period between welding start (W_S) and welding end (W_E) plus Zone B of the cooling period between martensite formation start (M_S) and finish (M_F) were used for relating to the tensile strength (σ_T, kgf/mm^2) of welded joints, because the AE counts at Zone A result primarily from the plastic deformation during welding and those at Zone B primarily from the martensitic phase transformation during cooling and then the cumulative total AE counts at Zone A+B should be more intimately as a whole correlated to the welded joint properties[4,5]. The correlated history graphs as those in Fig. 3 were made according to every welding condition and used for analysis of each weldment and AE measurement.

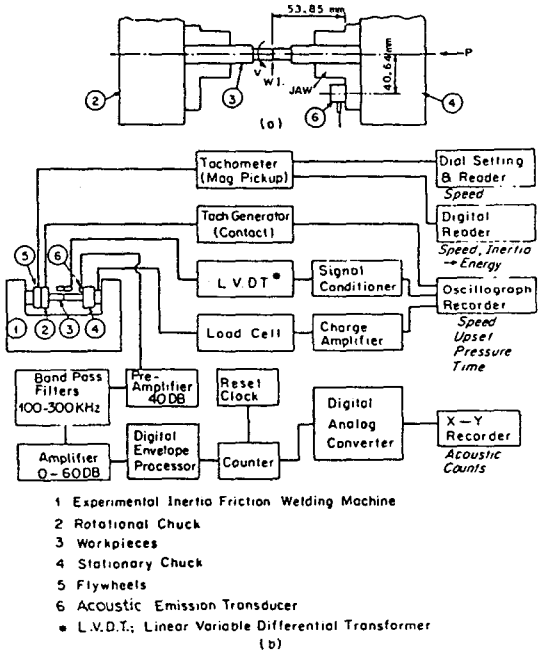

Fig.2 (a) AE transducer location.

(b) Block diagram of AE monitoring equipment and welding parameters measuring apparatus.

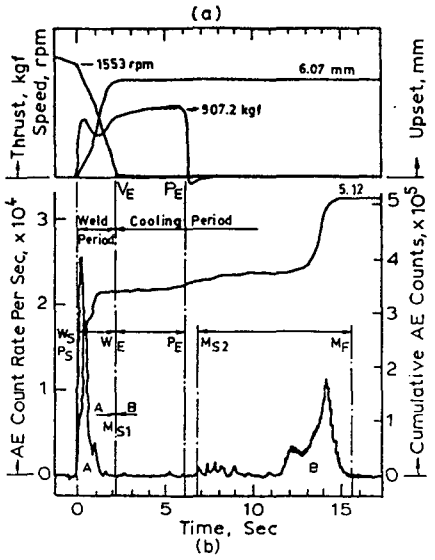

Fig.3 History of welding parameters and AE measurement in inertia friction welding.

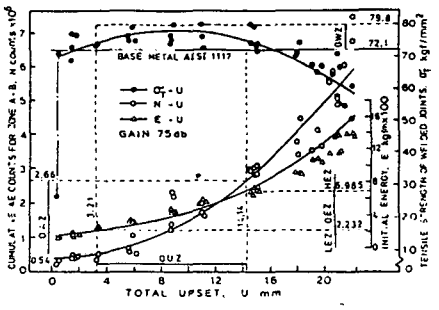

Fig.4 Correlation between cumulative total AE counts for Zone A+B and total upset relating to initial energy and friction weld strength of 9.525 mmΦ bar-to-bar welds of AISI 4140 to 1117 steels (I=0.236 kgfm^2, p=12.7 kgf/mm^2, V=937 to 3450 rpm, E=116 to 1572 kgfm).

3. RESULTS AND DISCUSSIONS

3.1 Effects of Total Upset on Weld Strength and AE Counts

In order to investigate the possibility of AE techniques application to the quality evaluating of the continuous drive type friction welding as well as the inertia (or flywheel) type friction welding, the effects of total upset (U) or time (T) on cumulative AE counts (N) relating to weld strength (σ_T) should be investigated, because the continuous drive friction welding is controlled in production primarily with the upsets (for heating and upsetting) or welding times (for heating and upsetting) or welding times (for heating and upsetting)under the selected rotational speed and pressures (for heating and upsetting) as welding conditions[1),2)].

It is known that the tensile strength of welded joint has dependence upon the upset amount (or welding time)[9)], which is correlated to the initial energy[1),2)].

Each initial energy (E, kgf·m) was calculated by the following formula[1)] at the selected inertia (I, kgfm^2) and rotating speed (V, rpm) :

$$E = IV^2/1787.3$$

As the total upset (U) increases in Fig. 4, the tensile strength (σ_T) of welded joints varies parabolically, while the initial energy (E) increase is related eventually to the total upset (U) increase as an exponential function. These properties are very similar to Hasui, et al.'s report[10)] on continuous drive friction welding of sulphurized free machining steel and Oh's[9)] on continuous drive friction welding of dissimilar materials (Si-Cr alloy steels to high Ni-Cr alloy steels).

The experimental data points for σ_T-U and E-U relationships were reliably fitted to the parabolic and exponential curves, respectively by the least squares method, resulting in the mean % errors of 4.23% for σ_T-U curve and 9.47% for E-U curve with high reliability at 95% confidence level. And such curves were better fitted with smaller errors than any other else in several trials for better curve fitting. It is found in Fig. 4 that the optimum total upset zone (OUZ) is 3.21 through 14.14 mm by the E-U curve, within which the welded joints have a tensile strength with the joint efficiency more than 100%.

In the meantime, it was found that an increase of total upset (U) results in an increasing cumulative total AE counts (N, for Zone A+B) along a quadratic curve, to which all the experimental data points were reliably fitted by the least squares method and the mean % error of the fitted curve was 14.1%, in a case when the curve has also reliability at 95% confidence in the lack of fit test[3),5)].

Thereby, as shown in Fig. 4, it was confirmed that, for getting the weld strength with the joint efficiency more than 100% as indicated by σ_T-U curve and base metal strength line in friction welding of AISI 4140 to 1117 steels (9.53 mmΦ), not only the optimum total upset zone (3.21 through 14.14 mm) can be obtained at the same-optimum initial energy zone (OEZ, 223.2 through 698.5 kgfm) by the E-U curve, but also the optimum AE zone (OAZ, 0.54×10^6 through 2.66×10^6 counts) can be obtained at such an OUZ by the N-U curve at the same time. This OAZ is coincident with the former report[3),5),8)].

Thus, it seems that the weld strength with the joint efficiency more than 100% in the continuous drive type friction welding as well as the inertia type can be also and evaluated in process by the cumulative total AE counts through total upset (but, actually, by heating upset and forging upset in the case of continuous type friction welding).

3.2 Effects of Welding Time on Weld Strength and AE Counts

For such reason as mentioned in the section 3.1 and for the additional verification for possibility of AE techniques application to the continuous drive type friction welding, the effects of welding time were also examined. The experimental results with the same materials and welding conditions as those in Fig. 4 are shown in Fig. 5.

It is certain in Fig. 5 that the weld strength (σ_T, tensile strength), cumulative total AE counts (N) and total upset (U) are all correlated cubically to welding time (T). So that, their experimental data points were fitted to each cubic curve, with the result that the reliability is kept at 95 % confidence level, too. And then, at the same total upset zone (OUZ) as that in Fig. 4, the optimum welding time zone (OUZ) is obtained by the U-T curve as 1.69 through 3.18 sec, at which the OAZ of 0.56×10^6 through 2.62×10^6 counts as well as the weld strength with the joint efficiency more than 100 % can be obtained at the same time through the N-T and σ_T-T curves, respectively. This OAZ by the welding time effects is also coincident with that in Fig.4.

Thus, it seems again that such cumulative total AE counts within the OAZ do indicate the weld strength monitored with the joint efficiency more than 100 % for friction welding of such same materials pairs and same welding conditions, and that this

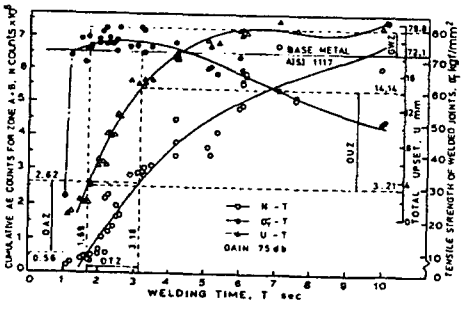

Fig.5 Correlation between cumulative total AE counts for Zone A + B and welding time relating to total upset and friction weld strength 9.525mmϕ bar-to-bar welds of AISI 4140 to 1117 steels (I = 0.236 kgfm², p = 12.7 kgf/mm², V = 937 to 3450 rpm, E = 116 to 1572 kgfm)

non-destructive test method of friction weld quality monitoring using AE techniques can be applied in continuous drive type friction welding as well as flywheel type.

3.3 Relationship between Weld Strength and Total AE Counts for Zone A+B

Fig.6 shows the relationship between the inertia friction weld strength and total AE counts for Zone A+B of friction welded joints of 9.3 mmϕ bars AISI 4140 to AISI 1117 steels. For comparison the cases of the weld of 25. 4mmϕ (3. 8mm wall) tubes AISI 1020 to AISI 304 stainless steels and 9.3 mmϕ bars AISI 4140 to AISI 12L14 steels are also given in Fig.6 Regarding to the optimum AE zone (OAZ) for each weld, the OAZ-1 in the case of the weld of AISI 4140 to AISI 1117 is the widest (0.5×10^6 through 2.5×10^6), because of more carbon contents in them and also the martensite-forming-stabilizer Cr content in AISI 4140 resulting in their excellent hardenability. This OAZ-1 is well coincident with the GAZ-1 in the former reports[5),8)]. This means that those have a high reliability.

In the case of welding AISI 1020 to AISI 304 stainless steel tubes, they have especially the area (a) where strength is dropped and total AE count are very low even though they were welded at high speed level (2968 through 2984 rpm). Those welds were fractured on the boundary area between HAZ and base metal. This must be the dangerous weak points in the view of welding strength. So that, the OAZ-2(1.2×10^6 through 2.5×10^6 counts) in Fig.4 should be compensated to the AE range of C-OAZ-2(1.2×10^6 through 1.9×10^6 counts) for attaining to the GWZ (good welding zone with the joint efficiency more than 100%) for safety quality monitoring and for practical use.

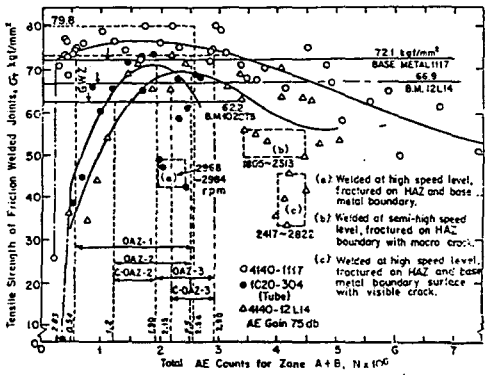

Fig.6 Relationship between inertia friction weld strength and total AE counts for Zone A + B or friction welded joints of 9.53mmϕ bars 4140 to 1117 steels, 4140 to 12L14 steels and 25.40mmϕ (3.18mm wall) tube 1020 to 304 stainless steels. AE Gain; 75db.

In the case of 4140-to-12L14 welds in Fig.6, they also have the dropped strength and lowered total AE counts areas (b) and (c) much scattered from the fitted curve exceptionally. The welds in the area (b) welded at semi-high speed level (1805 through 2313 rpm) were fractured on HAZ boundary surface with macro- or micro-crack (as shown in Fig.7). And also the welds in the area (c) welded at high speed level were fractured on the HAZ and base metal boundary surface with visible crack, and with macro or micro crack (as shown in Fig.7 (d) and (e) observed by EPMA X-ray images). To avoid these weld defects, the OAZ-3 of AE counts with the range of 1.90×10^6 through 2.90×10^6 counts should be compensated to the C-OAZ-3 with the range of 2.15×10^6 through 2.90×10^6 counts for safety quality monitoring and for practical use, in Fig.6.

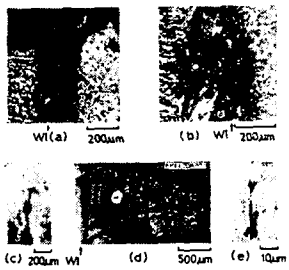

(a) Non-welded periphery of 4140-1117 joint welded at the lowest speet lever (937rpm).
(b) Crack and center defects of 4140-1117 joint welded at the lowest speed lever (937rpm).
(c) Macro crack on HAZ boundary surface of 4140-12L14 joint welded at *somi-high speed level (2313rpm).*
(d) Macro crack at boundary area of HAZ and base metal of 4140-12L14 joint welded at high speed level (2617rpm). (EPMA X-ray image, BEI(COMPO), 20 kV).
(e) Micro crack kiscontinuities on HAZ boundary of 4140-12L14 joint welded at high speed level (2617rpm). (EPMA X-ray image, SEI, 20 kV).

Welding conditions:I=0.236kgf · m^2, p=12.7kgf/mm^2, n=as above.

Fig.7 Macro and micro photos, and EPMA X-ray images for the discontinuities of the intertia welded joints welded at different speed levels.

The empirical equations of σ_T-N for 4140-1117, 1020-304 and 4140-12L14 welds are given as the following, computed by the polynomial regression analysis, calculating the equation adequacy by the error analysis[5]:

For 4140-to-1117 (9.53 *mm dia.) welds:*

$\sigma_T = -154.54\times10^{-21}N^3 - 2.3807\times10^{-12}N^2 + 6.6381\times10^{-6}N + 71.39$,
$(0.320\times10^6 \leq N \leq 7.447\times10^6$, Eq. adeq.
: mean % error 4.24) (1)

For 1020-to-304 (25.4 mmφ, 3.18mm wall tubes) welds:

$\sigma_T = -14.779\times10^{-12}N^2 + 54.917\times10^{-6}N + 19.94$,
$(0.515\times10^6 \leq N \leq 2.649\times10^6$, Eq. adeq.
: mean % error 8.02) (2)

For 4140 12L14 (9.53 mm dia.) welds:

$\sigma_T = 1.9987\times10^{-16}N^3 - 21.274\times10^{-12}N^2 + 66.801\times10^{-6}N + 4.12$,
$(0.442\times10^6 \leq N \leq 5.041\times10^6$, Eq. adeq.
: mean % error 9.34) (3)

Thus, by the above empirical equations of the σ_T-N relationship for the welded joints(AISI 4140-1117, 1020-304 and 4140-12L14), the general empirical equation form can be modeled as the following cubic ($a\neq0$) or parabolic ($a=0$) equation depending on materials:

$$\sigma_T = aN^3 + bN^2 + cN + d \quad (4)$$

3.4 Comparison between Empirical and Calculated Equations and 95% Confidence Tests

Fig.8 shows the comparison between the calculated equations[8] and the empirical equations (1) & (2) : Such calculated equations derived from the combination of empirical σ_T -*n* and *N*-*n* are as follows[8],

4140-1117 : $\sigma_{Tn} = -731.94 \times 10^{-6}N^{0.7466} + 209.23 \times 10^{-3}N^{0.37688} + 46.55$
$(0.283\times10^6 \leq N \leq 7.356\times10^6$, Mean % Diff. 0.6%) (5)

1020-304 : $\sigma_{Tn} = -13.368 \times 10^{-6}N^{1.0871} + 73.813 \times 10^{-3}N^{0.54856} - 30.18$
$(0.895\times10^6 \leq N \leq 2.484\times10^6$, Mean % Diff. 2.02%) (6)

The maximum mean % difference is only 2.05%, showing a high reliability.

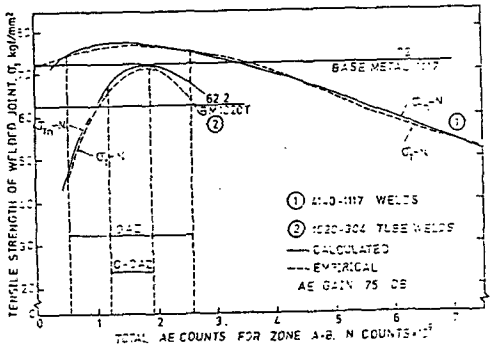

Fig.8Comparison between calculated and empirical equations for friction weld strength versus total AE counts of 9.535 mmϕ bar-to-bar(AISI 4140 to 1117) and 25.4 mmϕ(3.185mm wall) tube-to-bube (AISI 1020 to 304S.S) welds.

Table 3 ANOVA table for testing the lack of fit on the empirical (σ_{Tn}-N, % difference 0.60) equation models of 4140-1117 welds.

SOURCE	SUM OF SQUARES	DEGREE OF FREEDOM	MEAN SQUARE	F - RATIO
RESIDUAL	6.2478×10^{12}	14		
PURE ERROR	9.0123×10^{11}	4	2.2531×10^{11}	
LACK OF FIT	5.3466×10^{12}	10	5.3466×10^{11}	2.37
REMARKS	FROM F-TABLE, $F_{10,\ 4,\ 0.05} = 5.96$ (95% CONFIDENCE)			

For their 95% confidence examination, in the case of 4140-1117 welds, the residual sum of squares for the weld strength are computed statistically, and the ANOVA table for testing the lack of fit is calculated as in Table 3. The calculated F-ratios for the lack of fit for both the empirical equations at full range and OAZ-1 of AE and the calculated equation are 1.44, 0.13 and 0.13 which are much smaller than the corresponding values of 3.09, 19.36 and 19.36, respectively from the F-table at 95 percent confidence level. This analysis suggests that not only there is no great danger of lack of fit between all the postulated models and the experimental data in this study, but also it seems possible to evaluate the weld strength quantitatively in real time during the process of production by the acoustic emission techniques[3,4,5,1,8] more reliably than by the conventional methods[9].

4. CONCLUSIONS

The results obtained in the study on Development of Real-Time Quality Evaluation of Friction Welding by Acoustic Emission are as follows:

(1) The weld strength can be quantitatively and usefully evaluated or controlled in real time of process by using AE techniques because it was confirmed experimentally and quantitatively that the friction weld strength and the total acoustic emission counts have the correlation between them, and the relationship model is expressed as

$\sigma_T = aN^3 + bN^2 + cN + d$, (depending on materials, a=0),

whose maximum mean % difference from the calculated model (σ_{Tn}) is 2.05%, and which has a high reliability, and can be used for inprocess real-time evaluating or monitoring of friction weld strength as a nondestructive evaluating method using AE techniques.

(2) It was confirmed again statistically by error analysis and lack-of-fit testing that the empirical equations for the relationship between the weld strength and the total AE counts computed by the regression analysis using the least squares method have also a reliability at 95% confidence level.

REFERENCES

1) AWS: Welding Handbook, Vol.3, pp.240, AWS, Miami, 1980.

2) JFWRC: Friction Welding, pp.57, 139, Edited by A. Hasui, Corona, Japan, 1979.

3) S.K.Oh: Friction Weld Strength Analysis by Acoustic Emission Techniques(1), J. of KSME, Vol.22, No.3, pp.184-190, 202, 1982.

4) K.K.Wang, S.K.Oh, G.R.Reif: In-Process Quality Detection of Friction Welds Using Acoustic Emission Techniques, Proc. 63rd Annual AWS Convention, Session 5-A(Apr.27, 1982). Welding Journal of AWS, Vol.61, No.9, September, Welding Research Supplement 312-316-s, 1982.

5) S.K.Oh, A.Hasui, T.Kunio, K.K.Wang: Effects of Initial Energy on Acoustic Emission Relating to Weld Strength in Friction Welding, Transaction of JWS, Vol.13, No.2, p.15-26, October, 1982, Proc. of 4th Int. Sym. of JWS, 4 JWS-V-8, Nov. 24-26, pp.713-718, 1982.

6) K.K.Wang, S.Ahmed: Ultrasonic Detection of Weld Strength for Dissimilar Metal Friction Welds, Proc. of 4th North American Metalworking Research Conf., pp.384, 1976.

7) S.Ahmed: Ultrasonic Detection of Weld Strength, A Technical Report, Cornell University, USA, 1975.

8) S.K.Oh, K.K.Wang: Effects of Welding Parameters on Weld Strength and Acoustic Emission in Friction Welding, Proc. of the Korean Society of Marine Engineers(Apr. 1982), J. of KOSME, Vol.7, No.1, pp.21-31, 1983.

9) S.K.Oh: Study on Friction Welding of Valve Materials-On Improving the Friction Weld Quality for Exhaustive Valve Materials SUH3-SUH31, J. of KSME, Vol.14-3, pp.221-232, 1974.

10) A.Hasui, S.Wakida: Friction Welding of Sulphur Free Machining Steel, Transactions of JWS, 12-1(April 1981), pp.8-13.

APPENDICES :

- Real-Time Evaluation of Automatic Production Quality Control for Friction Welding Machine : Report 2

Abstract

Both in-process quality control and high reliability of the weld is one of the major concerns in applying friction welding to the economical and qualified mass-production. No reliable nondestructive monitoring method is available at present to determine the real-time evaluation of automatic production quality control for friction welding machine.

This paper, so that, presents the experimental examinations and statistical quantitative analysis of the correlation between the initial cumulative counts of acoustic emission(AE) occurring during plastic deformation period of the welding and the tensile strength of the welded joints as well as the various welding variables, as a new approach which attempts finally to develop an on-line (or real-time) quality monitoring system and a program for the process of real-time friction welding quality evaluation by initial AE cumulative counts.

As one of the important results, it was well confirmed that the initial AE cumulative counts were quantitatively and cubically correlated with reliability of 95% confidence level to the joint strength of the welds, bar-to-bar (SCM4 to SUM31, SCM4 to SUM24L) and that an AE technique using initial AE counts can be reliably applied to real-time strength evaluation of the welded joints, and that such a program of the system was well developed resulting in practical possibility of real-time quality control more than 100% joint efficiency showing good weld with no micro-structural defects.

Table 1 Chemical composition and tensile strength of base metals

Materials	Chemical composition (wt %)									T.S*
	C	Mn	P	S	Pb	Cr	Mo	Ni	Si	σ_T
SCM4	0.38	0.75	0.04	—	—	0.80	0.15	—	0.20	113.4
SUM31	0.17	1.00	0.04	0.08	—	—	—	—	—	72.0
SUM24L	0.15	0.85	0.04	0.26	0.15	—	—	—	—	66.9

Table 2 Friction welding conditions (Inertia type)

Materials combination	Diameter D, mm	Moment of inertia I, kgfm²	Initial rotating speed n, rpm	Axial pressure p, kgf/mm²	Initial energy E, kgfm
Bar-to-bar SCM4-SUM31	9.525	0.118	1136	12.7	85
		0.236	937~3450		116~1572
		0.472	883~2572		206~1747
Bar-to-bar SCM4-SUM24L	9.525	0.236	1132~2822	12.7	169~1052

Table 3 ANOVA table for testing the lack of fit on the empirical N_A-n equation ($M\%E=13.09$) of SCM4-SUM31 welds

Source	Sum of squares	Degree of freedom	Mean square	F-ratio
Residual	7.4606×10^{11}	38		
Pure error	7.9962×10^{10}	8	9.9953×10^{9}	
Lack of fit	6.6610×10^{11}	30	2.2203×10^{10}	2.22
Remarks	From F-table: $F_{30,8,0.05}=3.08>2.22$ (95% confidence)			

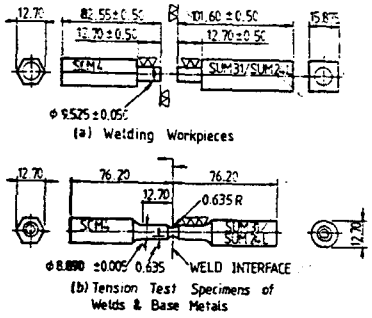

Fig. 1 Dimensions(mm) of welding workpieces and tension test specimens

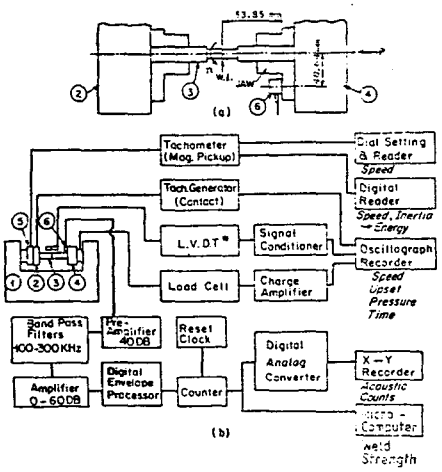

① Experimental inertia friction welding machine
② Rotational chuck
③ Workpieces
④ Stationary chuck
⑤ Flywheels
⑥ Acoustic emission transducer
* L.V.D.T.; Linear variable differential transformer

Fig. 2 (a) AE transducer location
(b) Block diagrams of welding-parameters measuring-apparatus, AE monitoring equipment and computer-aided-strength-evaluation

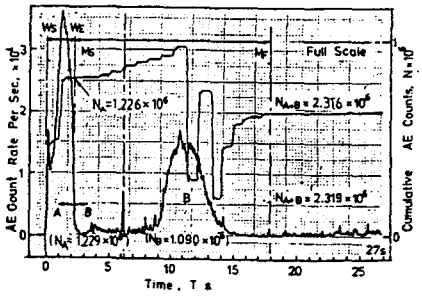

Fig. 3 Typical histories of acoustic emissions (AE count rate, cumulative AE counts) versus time(from welding start W_s to welding end W_E and during cooling period M_S to M_F) in inertia friction welding of SCM4 to SUM24L steels(ϕ 9.525mm) (I=0.236kgfm², AE gain 75dB)

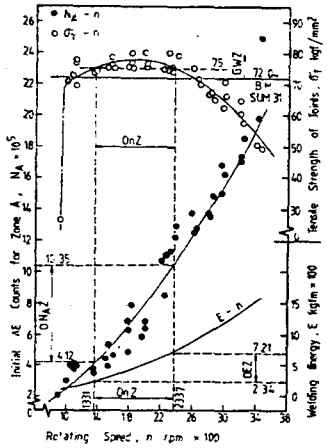

Fig. 4 Effects of rotating speed and welding energy on initial AE counts and weld strength for ϕ 9.525mm bar-to-bar welds of SCM4 tc SUM31 steels. AE gain; 75dB.

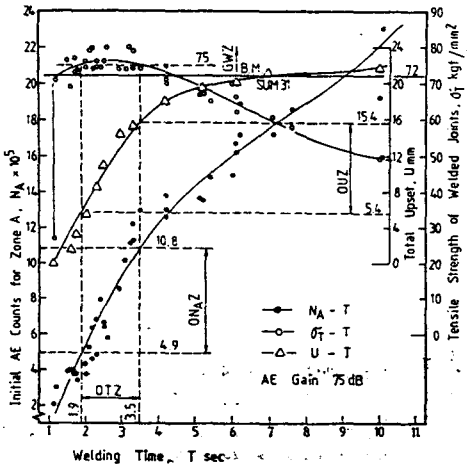

Fig. 5 Effects of welding time and total upset on initial AE counts and weld strength for ϕ9.525 mm bar-to-bar welds of SCM4 to SUM31 steels

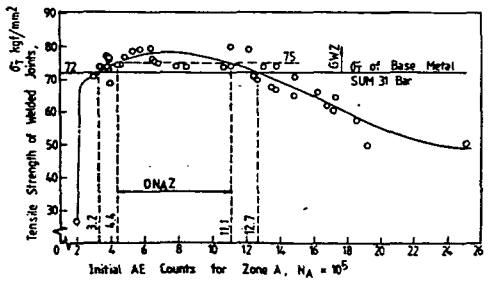

Fig. 6 Correlation between initial AE counts for Zone A (plastic deformation) and weld strength of friction welded joints of ϕ 9.525mm bars, SCM4 to SUM31 steels AE gain; 75dB.

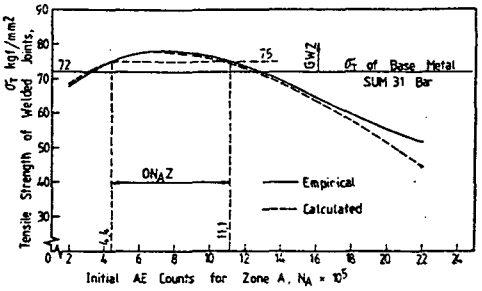

Fig. 7 Comparison between calculated and empirical equations for friction weld strength versus initial AE counts of ϕ 9.525mm bar-to-bar welds (SCM4-SUM31). AE gain; 75dB.

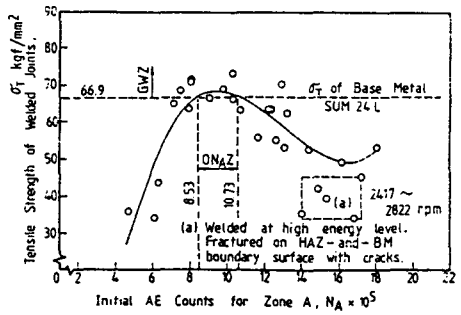

Fig. 8 Correlation between initial AE counts for zone A (plastic deformation) and welded joints of ϕ 9.525mm bars, SCM4 to SUM24L steels. AE gain; 75dB

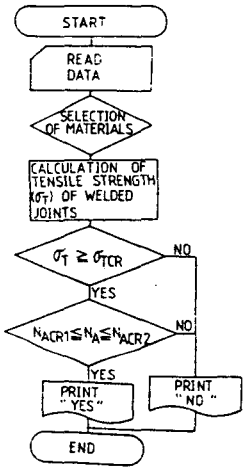

Fig. 9 Block diagram of real-time evaluation process chart for automatic production quality control of friction welding machine by initial AE cumulative counts

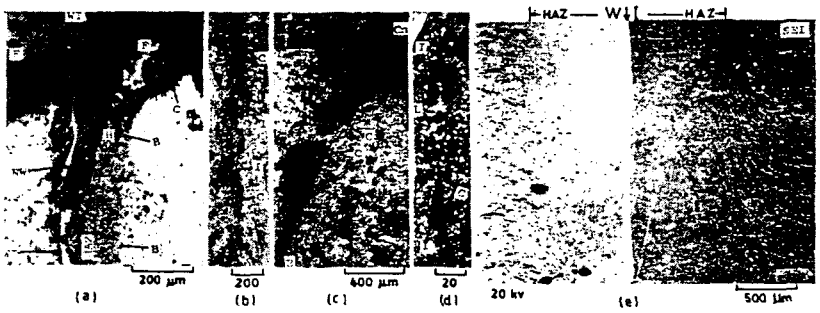

(a) Flash corner crack of SCM4-SUM31 welds, welded at low level of E=106kgfm, N_A=2.05 $\times 10^5$ounts, σ_T=67.99kgf/mm²

(b) Center crack of SCM4-SUM24L welds, welded at low level of E=169kgfm, N_A=8.09$\times 10^5$ counts, σ_T=65.37kgf/mm²

(c) Flash corner crack of SCM4-SUM24L welds welded at high level of E=904kgfm, N_A=1.406 $\times 10^6$ counts, σ_T=54.90kgf/mm²

(d) HAZ boundary periphery vicinity crack of SCM4-SUM24L welds, welded at high level (same as(c))

(e) Good weld with no defects of SCM4-SUM24L welds, showing re-orientation of fine lead and sulphide inclusions along spiral metal flows welded at optimum level of E=346kgfm, N_A=1.02$\times 10^6$ counts, σ_T=67.87kgf/mm²

Fig. 10 Micro-photographs ((a) (d)) of weld cracks and EPMA X-ray image (e) of welded zone in friction welding at the low or high level welding energy relating to cumulative initial AE counts: (I= 0.236kgfm², P=12.7kgf/mm²)

· Real-Time Evaluation of Friction Welding Quality of Small-Type Hydraulic Valve Spool by Acoustic Emission : Report 3

Abstract

Both in-process quality control and high reliability of the weld is one of the major concerns in applying friction welding to the economical and qualified mass-production. No reliable nondestructive monitoring method is available at present to determine the real-time evaluation of automatic production quality control for friction welding of special hydraulic valve spool of 16mm in diameter.

This paper, so that, presents the experimental examinations and statistical quantitative analysis of the correlation between the initial cumulative counts of acoustic emission(AE) occurring during plastic deformation periods of the welding and the tensile strength and other properties of the welded joints of ϕ16 valve spool as well as the various welding variables, as a new approach which attempts finally to develop real-time quality monitoring system for friction welding.

Table 1 Chemical composition of SCM415(wt%)

Material	C	Si	Mn	P	S	Ni	Cr	Mo
SCM415	0.16	0.25	0.73	0.009	0.007	–	0.99	0.17

Table 2 Mechanical properties of SCM415

Material	Tensile Strength σ(kgf/mm^2)	Elongation ε(%)	Reduction of Area ϕ(%)	Hardness H_v	Heat Treat.
SCM415	50.5	32	58	85	863℃ Annealed
	85	16	40	300	850℃ Oil-Quenched, 200℃ Tempered Air Cooling

Table 3 AE instrumentation and operating parameters

Transducers	PZ Type R-15 150kHz resonance frequency
Pre-amplifier	Model 1220A 40dB fixed gain 100-300kHz filter
Post-amplifier	40dB gain
Threshold	1.0V

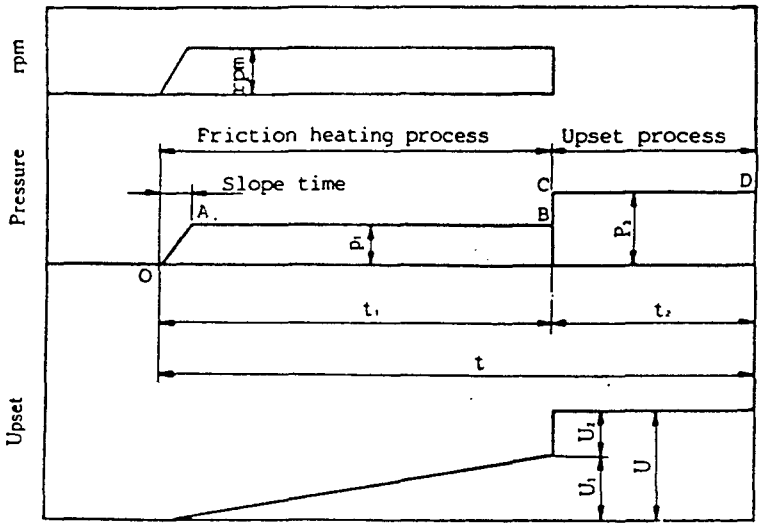

P_1 : Friction heating pressure (kgf/mm²)
P_2 : Upsetting pressure (kgf/mm²)
t_1 : Friction heating time (sec)
t_2 : Upsetting time (sec)
t : Total welding time (sec)
U_1 : Upset during heating time (mm)
U_2 : Upset during upsetting time (mm)
U_T : Total upset (mm)

Fig. 1 Schematic friction welding cycle (continuous drive brake type)

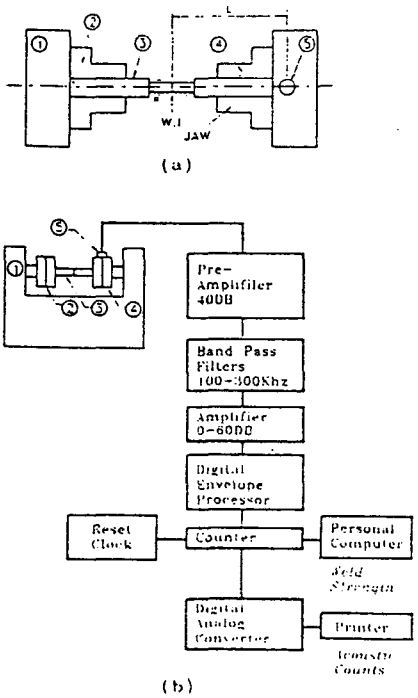

① Brake type friction welding machine
② Rotational chuck
③ Workpieces
④ Stationary chuck
⑤ Acoustic emission transducer

Fig. 2 (a) AE transducer location
(b) Block diagram of AE mointoring equipment and computer-aided-strength-evaluation

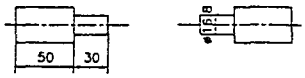

(a) Friction welding and AE test specimens of ϕ16.8 bar to bar

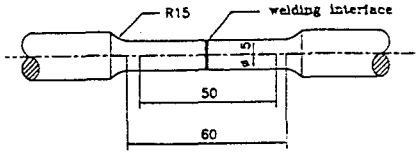

(b) Tension test and energy absorption specimens

Fig. 3 ϕ16.8 bar-to-bar specimen for manufacturing ϕ16 special valve spool

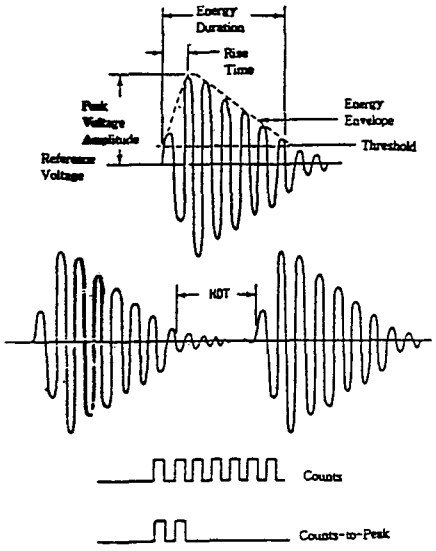

Counts(Example ; 7counts)
Amplitude(Example ; 66dB)
Duration(Example ; 361μs)
Counts-to-Peak(Example ; 2counts)

Fig. 4 Schematic illustration of AE event waveform and characteristics

$$N = (f/\alpha)\ln(Vp/Vt) \quad (1)$$

여기서

N ; ring down count

f ; 주파수, α ; 감쇠계수

Vp ; peak amplitude

Vt ; threshold voltage

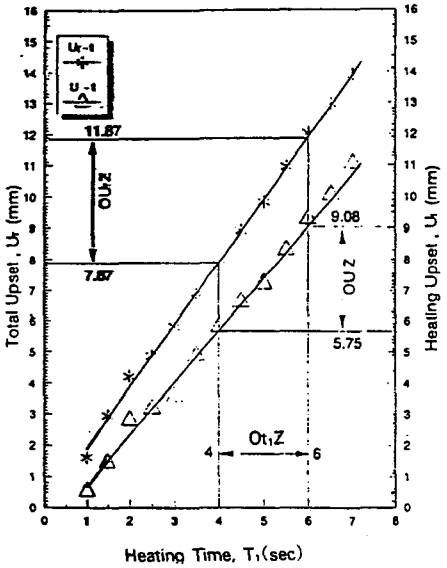

Fig. 5 U_T vs t_1 and U_1 vs. t_1 for φ16.8 bar-to-bar friction welding of SCM415)
Welding cond. : n=2,000rpm, P_1=9, P_2=15kgf/mm², t_1=1~7sec, t_2=4sec

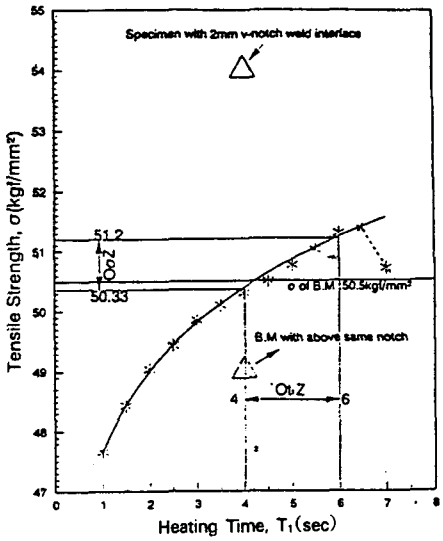

Fig. 6 σ vs. t_1 of friction welded joints of φ16.8 bar-to-bar of SCM415
Welding cond. : n=2,000rpm, P_1=9, P_2=15kgf/mm², t_1=1~7sec, t_2=4sec

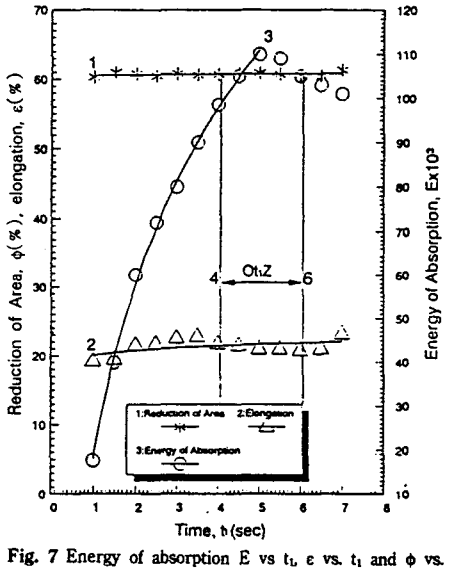

Fig. 7 Energy of absorption E vs t_1, ε vs. t_1 and φ vs. t_1 of friction welded joints of SCM415 φ16.8 bar-to-bar

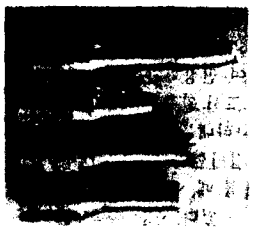

(a) Tensile fractured specimens

(b) Fracture surface of B.M.

(c) Ductile fracture of B.M.

(d) Fracture surface of weld interface

(e) Ductile fracture of W.I

(f) Brittle fracture of W.I

Fig. 8 Fractographs of tensile fractured base metal and weld interface of φ16.8 SCM415 bar-to-bar friction welding

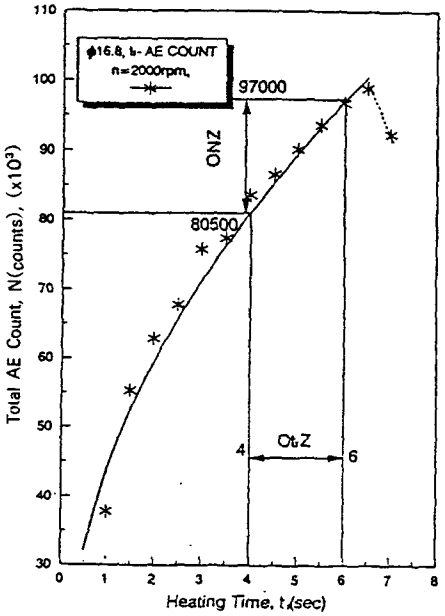

Fig. 9 N vs. t_1 *in friction welding of* φ16.8 *bar-to-bar of SCM415*
Welding cond. : n=2,000rpm, P_1=9, P_2=15kgf/mm², t_1=1~7sec, t_2=4sec

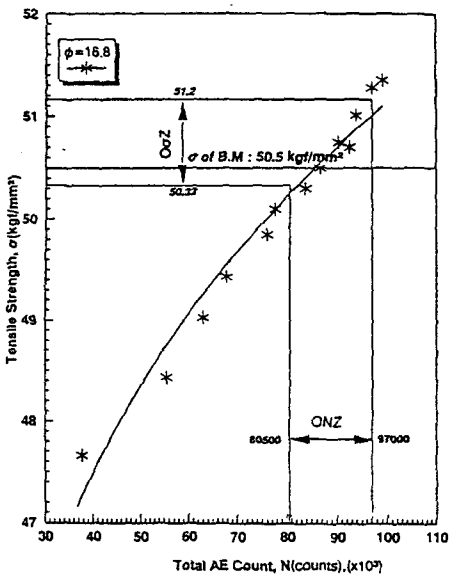

Fig. 10 σ vs. N in friction welding of φ16.8 bar-to-bar of SCM415
Welding cond. : n=2,000rpm, P_1=9, P_2=15kgf/mm², t_1=1~7sec, t_2=4sec

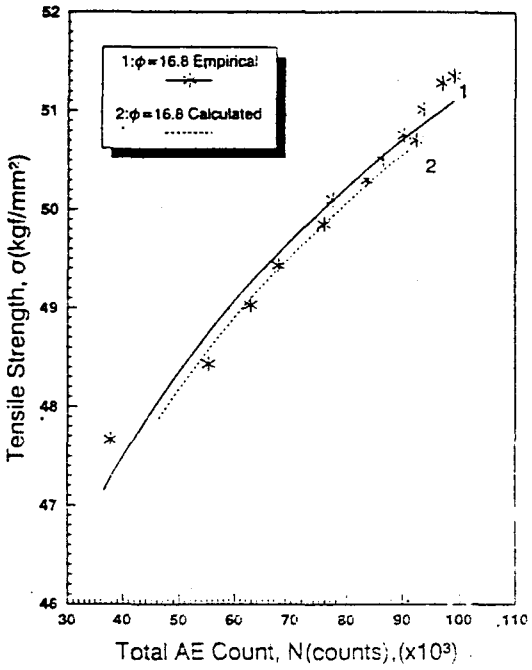

Fig. 11 Comparison between empirical and calculated equations for σ vs. N in friction welding of SCM 415 φ16.8
Welding cond. : n=2,000rpm, P_1=9, P_2=15kgf/mm², t_1=1~7sec, t_2=4sec

φ16.8 weld of φ16 valve spool

Finished product of φ16 valve spool

L.H.S of φ16 V.S

L.H.S : longitudinal half section

Fig. 12 Appearance of weld, longitudinal half section and finished product of φ16 hydraulic valve spool

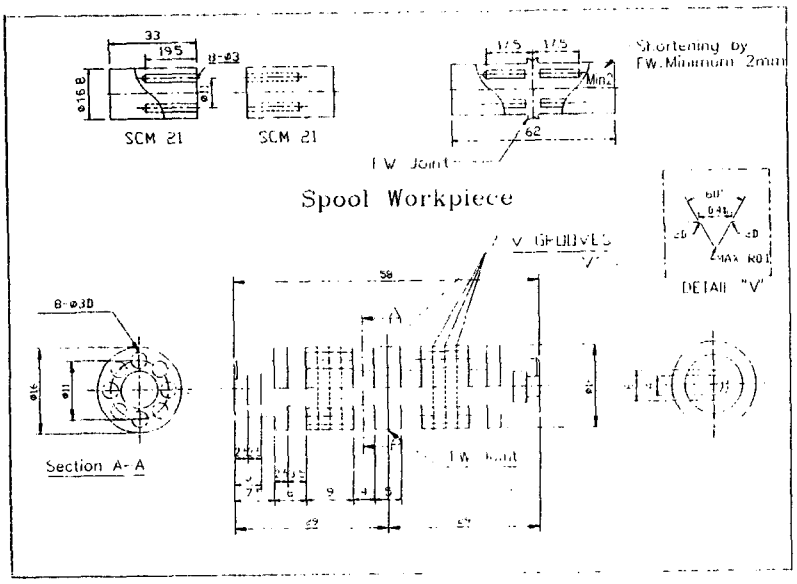

Fig.13 Drawing-1, Special hydraulic Valve Spool

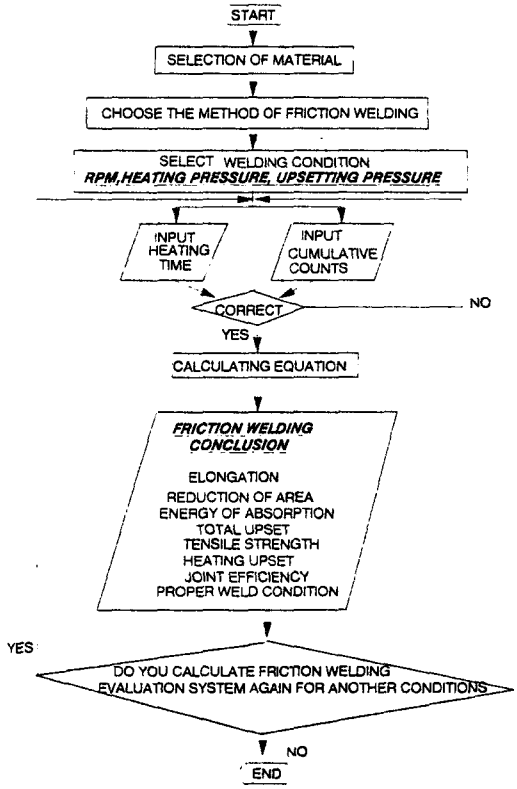

Fig.14 Process of frction welding evaluation system

- Study on Optimization of Friction Welding of Cr-Mo Steels and Evaluation of Weld Strength by Acoustic Emission : Report 4
  Fig.1, Table 1, Fig.2

- A Study on Optimization of Bar-to-Bar Similar Friction Welding of Hydraulic Valve Spool Steels and the Fatigue Strength Properties and its AE Evaluation : Report 5
  Table 1, Fig.2

- A Study on Optimization of Bar-to-Bar Dissimilar Friction Welding of Hydraulic Valve Spool Steels and the Fatigue Strength Properties and its AE Evaluation : Report 6
  Table 1, Fig.2

- A Study on Optimization of Tube-to-Bar Dissimilar Friction Welding of Hydraulic Valve Spool Steels and the Fatigue Strength Properties and its AE Evaluation : Report 7
  Fig.1, Table 1, Fig.2

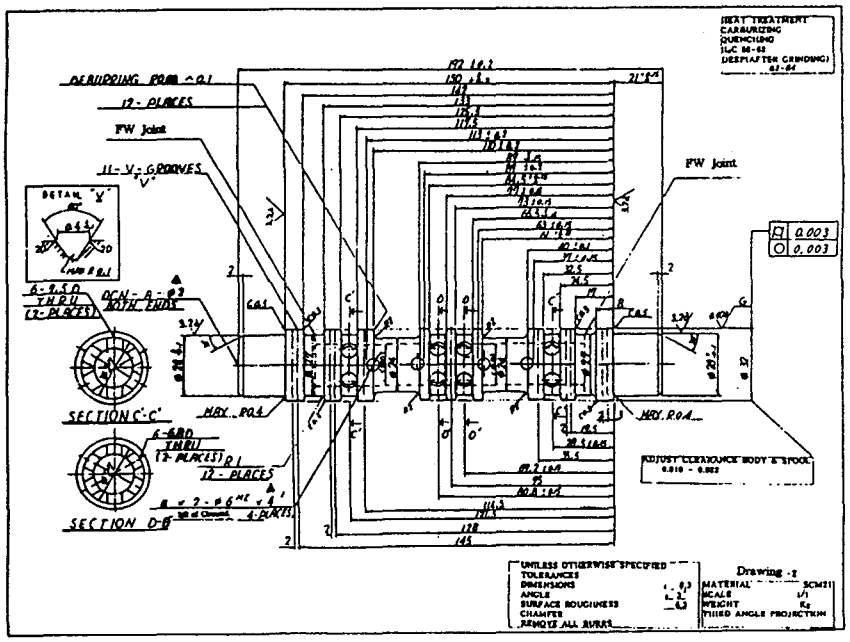

Fig.1 (Drawing 2) Special hydraulic valve spool of ϕ32(I.D. ϕ18)

Table 1 FRW cond. of Data-Base System for Similar or Dissimilar Welding Standardization of Various Hydraulic (/ Pneumatic) Valve Spools

Material			Heating Pressure P_1 (kg_f/mm^2)	Upsetting Puressure P_2 (kg_f/mm^2)	Heating Time T_1 (sec)	Upsetting Time T_2 (sec)	Rotating speed n (rpm)
Similar	Dia.						
SCM415	16.8	bar-to-bar	9	15	1~7	4	2000
SACM645	31.2		4	8	18~34	4	1600
	24		7	10	9~11	5	2000
SNCM220	31.2		5	10	8~20	4	1600
	24		7	10	6~10	5	2000
SCM435	31.2		4	8	18~34	4	1600
	24		7	10	8~12	5	2000
SCM415	31.2		4	8	19~25	4	1600
	24		7	10	6~9	5	2000
SACM645	36	tube-to-bar	5	10	10~24	4	1600
SNCM220	36		5	10	3~20	4	1600
SCM435	36		5	10	4~20	4	1600
SCM415	36		5	10	15~22	4	1600

Material			Heating Pressure P_1 (kg_f/mm^2)	Upsetting Puressure P_2 (kg_f/mm^2)	Heating Time T_1 (sec)	Upsetting Time T_2 (sec)	Rotating speed n (rpm)
Dissimilar	Dia.						
SCM415× SNCM220	31.2	bar-to-bar	5	10	9~15	6	1600
	24		7	10	4~7	5	2000
SCM415× SACM645	31.2		5	10	9~15	6	1600
	24		7	10	3~5	5	2000
SCM435× SNCM220	31.2		5	10	9~15	6	1600
	24		7	10	5~8	5	2000
SCM435× SNCM645	31.2		5	10	9~15	6	1600
	24		7	10	3~6	5	2000
SCM415× SNCM220	36	tube-to-bar	6	12	10~24	6	1600
SCM415× SNCM645	36		6	12	3~20	6	1600
SCM435× SNCM220	36		6	12	4~20	6	1600
SCM435× SNCM645	36		6	12	15~22	6	1600

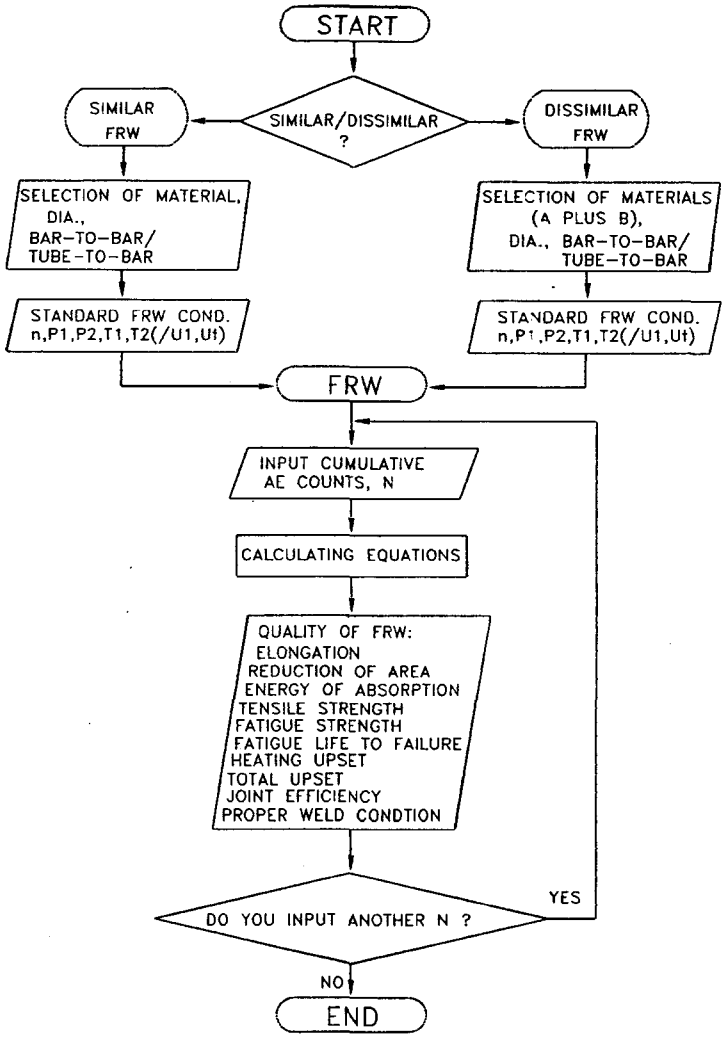

Fig.2 Block diagram of Real-Time Quality Evaluation System Process Chart for Similar or Dissimilar Friction Welding of Various Hydraulic (/Pneumatic) Valve Spools by Acoustic Emission Technique

ACKNOWLEDGEMENTS

This work(1993-1995) was supported by the '93 Cooperation Research Fund of Korea Science & Engineering Foundation for the project title(Serial No. 93-10-00-05-3) of "Development of Data-Base System for Friction Welding Standardization of Various Hydraulic (/Pneumatic) Valve Spools and the Real-Time Quality Evaulation by Acoustic Emission Techniques."